THE JOURNAL OF BIOLOGICAL CHEMISTRY VOL. 291, NO. 47, pp. 24364–24376, November 18, 2016

Psoralen and Ultraviolet A Light Treatment Directly Affects Phosphatidylinositol 3-Kinase Signal Transduction by Altering Plasma Membrane Packing*

Received for publication, April 27, 2016, and in revised form, September 17, 2016 Published, JBC Papers in Press, September 29, 2016, DOI 10.1074/jbc.M116.735126

Britt Van Aelst[‡], Rosalie Devloo[‡], Pierre Zachée[§], Ruben t'Kindt[¶], Koen Sandra[¶], Philippe Vandekerckhove[‖‡‡], Veerle Compernolle[‡‖‡‡], and Hendrik B. Feys[‡1]**

*From the [‡]Transfusion Research Center, Belgian Red Cross-Flanders, 9000 Ghent, Belgium, the [§]Department of Hematology, Hospital Network Antwerp, 2000 Antwerp, Belgium, the [¶]Research Institute for Chromatography, 8500 Kortrijk, Belgium, the [‖]Blood Service of the Belgian Red Cross-Flanders, 2800 Mechelen, Belgium, the **Department of Public Health and Primary Care, KULeuven, 3000 Leuven, Belgium, and the [‡‡]Faculty of Medicine and Health Sciences, Ghent University, 9000 Ghent, Belgium*

Edited by George Carman

Psoralen and ultraviolet A light (PUVA) are used to kill pathogens in blood products and as a treatment of aberrant cell proliferation in dermatitis, cutaneous T-cell lymphoma, and graft-*versus*-host disease. DNA damage is well described, but the direct effects of PUVA on cell signal transduction are poorly understood. Because platelets are anucleate and contain archetypal signal transduction machinery, they are ideally suited to address this. Lipidomics on platelet membrane extracts showed that psoralen forms adducts with unsaturated carbon bonds of fatty acyls in all major phospholipid classes after PUVA. Such adducts increased lipid packing as measured by a blue shift of an environment-sensitive fluorescent probe in model liposomes. Furthermore, the interaction of these liposomes with lipid order-sensitive proteins like amphipathic lipid-packing sensor and α-synuclein was inhibited by PUVA. In platelets, PUVA caused poor membrane binding of Akt and Bruton's tyrosine kinase effectors following activation of the collagen glycoprotein VI and thrombin protease-activated receptor (PAR) 1. This resulted in defective Akt phosphorylation despite unaltered phosphatidylinositol 3,4,5-trisphosphate levels. Downstream integrin activation was furthermore affected similarly by PUVA following PAR1 (effective half-maximal concentration (EC_{50}), 8.4 ± 1.1 *versus* 4.3 ± 1.1 μM) and glycoprotein VI (EC_{50}, 1.61 ± 0.85 *versus* 0.26 ± 0.21 μg/ml) but not PAR4 (EC_{50}, 50 ± 1 *versus* 58 ± 1 μM) signal transduction. Our findings were confirmed in T-cells from graft-*versus*-host disease patients treated with extracorporeal photopheresis, a form of systemic PUVA. In conclusion, PUVA increases the order of lipid phases by covalent modification of phospholipids, thereby inhibiting membrane recruitment of effector kinases.

Psoralens are linear furanocoumarins. Their heterocyclic aromatic core reversibly intercalates in nucleic acid clefts of cell nuclei (1). Absorption of ultraviolet A (UVA)[2] light excites the psoralen, supplying energy for covalent bond formation. When in the vicinity of nucleic acids, the reaction is primarily with pyrimidine moieties (2). This chemical addition is irreversible and prevents normal replication of DNA (3), explaining why severe phytophotodermatitis occurs in sun-exposed skin that has been in contact with psoralen-producing plants. This biostatic photochemistry is utilized in a pathogen inactivation technology (Intercept Blood System, Cerus Corp., Concord, CA) for plasma and platelet concentrates in transfusion medicine (4) where it prevents replication of potentially infectious pathogens transmitted from the donor to the blood product. In dermatology, PUVA is used to treat psoriasis, certain dermatoses, and cutaneous T-cell lymphoma (5). In these cases, the psoralen is administered topically or systemically followed by local or whole body UVA illumination. Treatment modalities are diverse and may differ by psoralen derivative and/or by doses of UVA light (6). Furthermore, PUVA is under clinical investigation for the treatment of multiple other diseases mostly involving uncontrolled cell proliferation (7). However, although broadly applied in medicine, the biochemical consequences of PUVA are poorly understood.

Psoralens are not clinically efficacious without UVA illumination, and despite its well documented photoreaction with DNA, PUVA photochemistry is not specific for this particular biologic target alone. In theory, photoexcited psoralens can react with many other common biomolecules. Therefore, the net effect of PUVA in a cellular milieu is unlikely to be restricted to consequences of its chemistry with solely DNA as was

* This work was supported by the Foundation for Research and Development of the Belgian Red Cross-Flanders Blood Service. The authors declare that they have no conflicts of interest with the contents of this article.

[1] To whom correspondence should be addressed: Transfusion Research Center, Belgian Red Cross-Flanders, Ottergemsesteenweg 413, 9000 Ghent, Belgium. Tel.: 32-9-244-56-58; E-mail: hendrik.feys@rodekruis.be.

[2] The abbreviations used are: UVA, ultraviolet A; PUVA, psoralen and ultraviolet A light; GVHD, graft-*versus*-host disease; ECP, extracorporeal photopheresis; Btk, Bruton's tyrosine kinase; Wm, wortmannin; NBD, 4-chloro-7-nitrobenzofurazan; 8-MOP, 8-methoxypsoralen; MeSADP, 2-(methylthio)adenosine 5-diphosphate ; IANBD, NBD iodoacetamide; ESI, electron spray ionization; PIP_2, bisphosphorylated phosphatidylinositol; PLC, phospholipase C; PI, phosphatidylinositol; PS, phosphatidylserine; PC, phosphatidylcholine; ALPS, amphipathic lipid-packing sensor; GPVI, glycoprotein VI; PAR, protease-activated receptor; GP, generalized polarization; $PI(3,4,5)P_3$, phosphatidylinositol 3,4,5-trisphosphate; $PI(4,5)P_2$, phosphatidylinositol 4,5-bisphosphate; PH, pleckstrin homology; P-Akt, phosphorylated Akt; PBMC, peripheral blood mononuclear cell; AUC, area under the curve; EC_{50}, effective half-maximal concentration.

acknowledged already in the late seventies (8). This random reaction with multiple biomolecules explains why the quest for understanding PUVA and optimizing therapies has been exceptionally challenging. For example, the systemic PUVA treatment modality ECP is used to treat cutaneous T-cell lymphoma, and although clinically successful (9), the mechanism of action has remained elusive ever since its first application. Researchers speculate that induction of apoptosis through DNA damage causes priming of the immune system. However, apoptosis induction alone is insufficient for the typical immunomodulation caused by PUVA (10, 11). Despite this uncertainty, ECP is used "off-label" for (auto)immune diseases including GVHD, bronchiolitis after stem cell transplantation, and Crohn's disease (12, 13). But without comprehension of definite biochemical mechanisms, both protocol uniformity and outcome variability will remain problematic.

Adduct formation of photoexcited psoralens with targets other than DNA (11, 14) is primarily with membrane components (15, 16). Psoralens efficiently partition into lipid bilayers (17, 18) where chemical reactions with double carbon bonds in unsaturated acyl chains take place (19, 20). As a consequence, rational hypotheses on the cell biological consequences of these modifications have been postulated (21, 22), but mechanisms explaining how membrane modifications exactly impact downstream cell signal transduction are unknown.

We chose platelets as model cells to study this because they have no nucleus, are easily isolated from whole blood, and contain a complex signal transduction machinery exemplary of key signaling processes in most eukaryotic cells. Furthermore, recent work has shown that PUVA significantly affects platelet function in an *in vitro* model of hemostasis (23). Our data now show that PUVA can inhibit signal transduction in the phosphatidylinositol 3-kinase (PI3K) pathway by preventing efficient plasma membrane recruitment of crucial effector kinases such as Akt (alternative name, protein kinase B) and Bruton's tyrosine kinase (Btk). Our findings are not restricted to platelets because T-lymphocytes in patient samples treated with ECP displayed attenuation of Akt phosphorylation as well.

Results

PUVA Modifies Phospholipids by Covalent Adduct Formation—Adducts between nucleic acids and psoralens like amotosalen or 8-methoxypsoralen (8-MOP) are formed in nucleated cells, but chemistry with (phospho)lipids has been described as well (15, 24). Mass spectrometry of platelet membrane extracts confirmed that PUVA causes amotosalen-lipid adduct formation, which was not found in control cells that were incubated with this psoralen in the dark (Fig. 1, *a* and *b*). All major phospholipid classes were targeted (Fig. 1*c*) provided they contained acyl chains with unsaturated carbon bonds (19). Fragmentation MS/MS spectra allowed identification of the main adducts that formed, and Fig. 1*d* depicts exemplary MS/MS data for PS(18:0/20:4), bisphosphorylated phosphatidylinositol (PIP_2)(18:0/20:4), amotosalen, and their UVA-dependent adducts.

PUVA Increases Lipid Order, Causing Inhibition of Protein Binding—Because photochemical addition of psoralens is to unsaturated carbon bonds, we hypothesized that PUVA causes changes in the order of lipid phases because this is typically controlled by acyl chain (un)saturation. To assess this, the environment-sensitive fluorescent probe NR12S (25, 26) was used in liposomes composed of PC(16:0/18:1). The emission peak of NR12S shifts blue in liquid-ordered liposomes, causing a rise in the generalized polarization (GP) value. In a validation experiment, this was demonstrated by addition of cholesterol, which is known to enhance lipid packing (Fig. 2*a*) (26). Ultraviolet A light treatment of amotosalen-containing liposomes caused apparent increases in lipid order similar to the addition of cholesterol, suggesting that phospholipid-amotosalen adducts tighten the acyl chain alignment.

Because disordered lipid microenvironments are important for protein-membrane interaction (27, 28), two archetypical membrane-adhering protein sequences, ALPS and α-synuclein (29, 30), were investigated for binding to PUVA-treated liposomes. As expected, the ALPS peptide efficiently bound to increasing concentrations of dark-treated control liposomes enriched in PC(18:1/18:1) but not PC(16:0/18:1) (Fig. 2*b*) (29). However, when the former were PUVA-treated, subsequent ALPS binding was inhibited to levels similar to the negative control. In a similar experiment, PUVA caused a significant decrease in α-synuclein binding to PS- and PC(18:1/18:1)-containing liposomes (Fig. 2*c*). Collectively, these data show that PUVA increases lipid order in liposomes and inhibits efficient binding of lipid packing-sensitive protein sequences.

PUVA Affects Akt and Btk Plasma Membrane Binding and Subsequent Signal Transduction—During platelet activation, essential interactions between membrane (phospho)lipids and cytoplasmic soluble proteins take place. These then relay signals to secondary messenger molecules, establishing successful primary hemostasis. Because PUVA affects protein interaction with model liposomes, we questioned whether this membrane binding of key cytoplasmic signaling proteins like Akt and Btk was intact in PUVA-treated platelets. To activate the initiating PI3K pathway in platelets, the collagen GPVI or the thrombin PAR1 was stimulated. Membrane binding of Akt and Btk was assessed by Western blotting of isolated membrane fractions. Significantly less Akt and Btk was found in PUVA *versus* paired untreated controls, pointing to defects in membrane binding in live cells as well (Fig. 3*a*). This defective binding moreover caused significant decreases in subsequent Akt phosphorylation, a major event in the PI3K signal transduction pathway (Fig. 3*b*) (31).

Binding of Akt and Btk to the activated membrane requires at least increased levels $PI(3,4,5)P_3$, which is produced by phosphorylation of PIP_2 by PI3K. Quantitative mass spectrometry on membrane extracts ruled out that $PI(3,4,5)P_3$ formation is abnormal in PUVA-treated resting and activated platelets (Fig. 4*a*). Furthermore, the relative amount of PIP_2-amotosalen adducts to total PIP_2 was only 1.2%, confirming that direct effects on the PI3K substrate were unlikely to cause decreased Akt membrane recruitment and phosphorylation. Furthermore, signal transduction in the concurrent phospholipase C (PLC) pathway was not affected by PUVA because the level of pleckstrin phosphorylation (Fig. 4*b*) and calcium release (data not shown) were normal in response to GPVI and PAR1 stimulation. Of note, platelet activation by another thrombin ana-

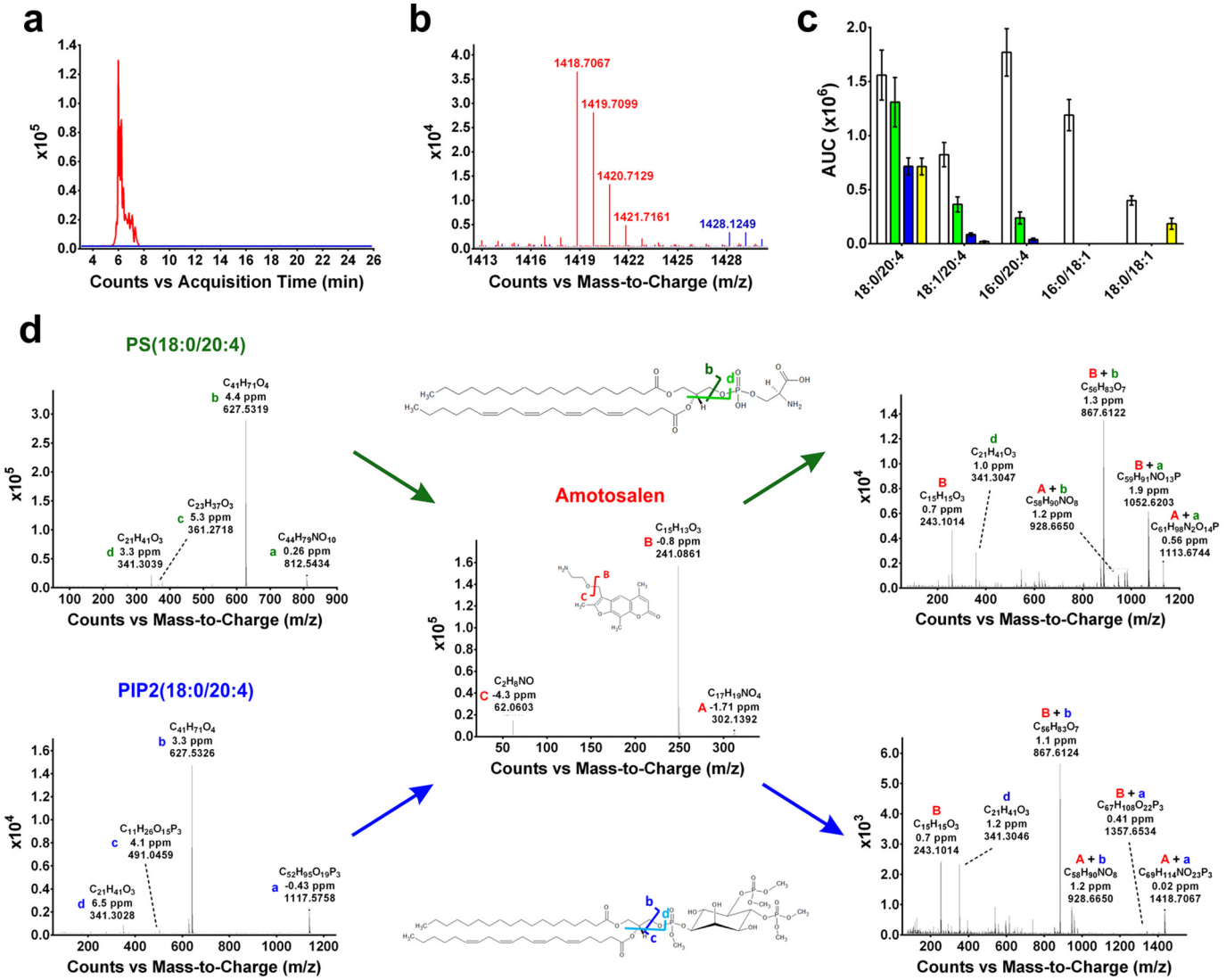

FIGURE 1. **Chromatography and mass spectrometry identified adducts between platelet membrane phospholipids and the psoralen amotosalen after PUVA.** *a*, extracted ion LC-MS chromatograms (*m/z* 1418.7073 ± 10 ppm) of PUVA-treated platelets (*red* tracing) indicate *de novo* formation of PIP_2(18:0/20:4)-amotosalen covalent adducts. Control extracts (*blue* tracing; overlaid) were not UVA-illuminated. *b*, exemplary accurate mass spectrum indicating covalent adducts of amotosalen and PIP_2(18:0/20:4) in the PUVA-treated (*red*) spectrum. Non-illuminated control (*blue*; overlaid) samples were devoid of adducts. *c*, amotosalen adducts were found in all major phospholipid classes using a search-by-mass strategy. Lipid-amotosalen adducts were confirmed by MS/MS analysis, and the AUC of the chromatographic peak was plotted for PC (*open bars*), phosphatidylethanolamine (*green*), PI (*blue*), and PS (*yellow*). Data represent mean, and *error bars* represent S.D. ($n = 4$). *d*, exemplary fragmentation MS/MS spectra of PS(18:0/20:4) (*green* annotations), PIP_2(18:0/20:4) (*blue* annotations), and amotosalen (*red* annotations) in the *left* and *middle panels*, respectively. Letter annotations refer to intact phospholipid (*a*) or amotosalen (*A*) and fragments of phospholipid (*b–d*) or amotosalen (*B, C*) corresponding to the structures given in the center of the panel. The two *right panels* depict characteristic adducts of these phospholipids with amotosalen.

logue that specifically targets PAR4 instead of PAR1 was not affected by PUVA and led to normal Akt phosphorylation (Fig. 4*c*). This is important because it demonstrates that the intrinsic potential to phosphorylate Akt is still present in PUVA-treated cells but depends on the kind of activatory input. Together, these data show that, despite generic adduct formation of psoralen with acyl chains, consequences for signal transduction are relatively selective and specific.

Platelet Integrin Activation Is Decreased by PUVA—Downstream of the investigated signaling circuit, platelets respond by activation of integrin $\alpha_{IIb}\beta_3$. Integrin activation of PUVA-treated platelets was investigated with flow cytometry using the conformation-sensitive monoclonal antibody PAC-1 (32). PUVA caused a significant decrease in integrin activation following stimulation with increasing doses of the thrombin PAR1 (effective half-maximal concentration (EC_{50}), 8.4 ± 1.1 *versus* 4.3 ± 1.1 μM) or the collagen GPVI (EC_{50}, 1.61 ± 0.85 *versus* 0.26 ± 0.21 μg/ml) receptor agonists (Fig. 5, *a* and *b*). In line with the Akt phosphorylation data, activation through PAR4 was normal (EC_{50}, 50 ± 1 *versus* 58 ± 1 μM) (Fig. 5*c*). As a control, the plasma membrane expression levels of the receptors GPVI and PAR1 was determined in flow cytometry and found to be normal (Fig. 5*d*).

PUVA Decreases Phosphorylation of Akt in T-lymphocytes from GVHD Patients—As a model for PUVA treatment of nucleated human cells, leukocytes were isolated from healthy consenting volunteers. The T-lymphocytes were activated by anti-CD3/CD28 beads. The effect of PUVA on T-cell activation

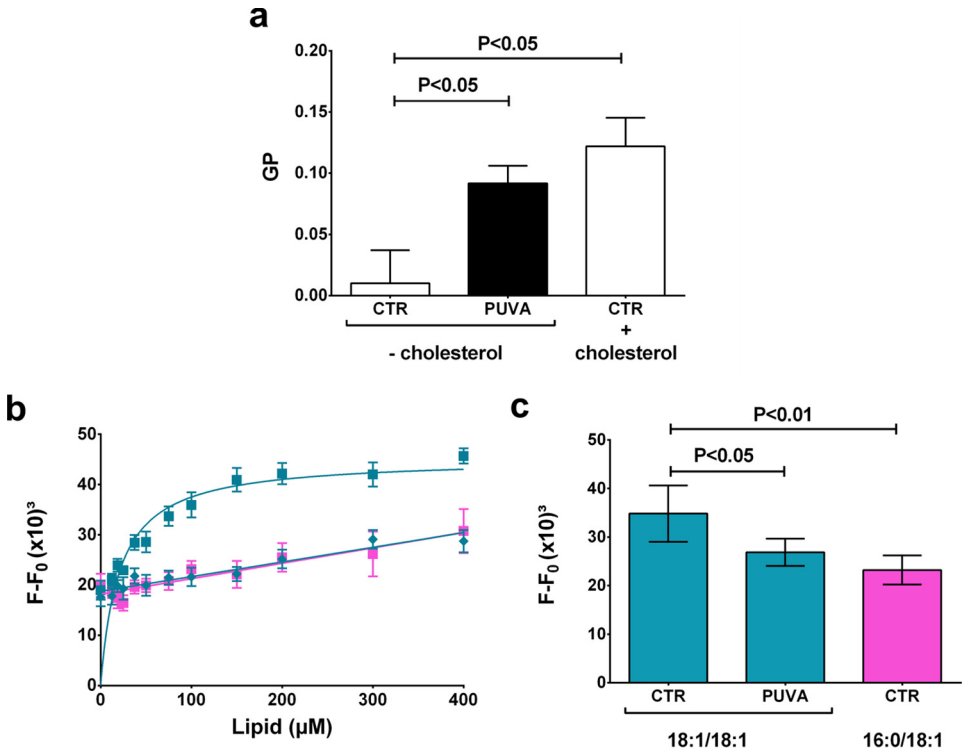

FIGURE 2. **PUVA treatment of liposomes increased the order of lipid phases and inhibited interaction with lipid packing-sensitive peptides.** *a*, the GP value is a relative measure of lipid order calculated from the fluorescence of the environment-sensitive probe NR12S at two emission wavelengths. Increased GP values indicate increases in lipid packing. Liposomes prepared from PC(16:0/18:1) were incubated with amotosalen and treated with UVA (*PUVA*; *closed bar*) or not (*CTR*; *open bar*). Cholesterol was added as a positive control for increased lipid order. Data are mean with S.D. as *error bars* ($n = 4$). *b*, binding of ALPS to PC(18:1/18:1)-enriched liposomes (*cyan*) or to PC(16:0/18:1) liposomes (*magenta*) is shown. All contained amotosalen and were left in the dark (■) or treated with UVA light (♦) prior to incubation with ALPS. The corrected peak fluorescence signal ($F - F_0$) of the covalently attached NBD moiety was used and is depicted as a function of lipid concentration. Data are mean with S.D. as *error bars* ($n = 6$). *c*, binding of α-synuclein to control liposomes (*CTR*) containing mainly 18:1/18:1 phospholipids (*cyan*) is compared with paired PUVA-treated counterparts and negative controls containing mainly 16:0/18:1 phospholipids (*magenta*). Also here, NBD was covalently attached, and the corrected peak fluorescence signal ($F - F_0$) is shown. Data are mean with S.D. as *error bars* ($n = 5$). *p* values are from one-way analysis of variance with Tukey's multiple comparison test.

was determined for 8-MOP and amotosalen in a paired experiment. The data show that both psoralens dose-dependently inhibited phosphorylation of Akt (Fig. 6, *a* and *b*), which was not caused by immediate cell death (data not shown). The data show that amotosalen was more efficient than 8-MOP, requiring lower concentrations to achieve half-maximal inhibition. To confirm whether Akt activation is affected in clinically relevant tissue, buffy coat cells from GVHD patients enrolled in a clinical efficacy study were collected before and after ECP. In these samples, Akt activation in T-lymphocytes was also significantly decreased (Fig. 6, *c* and *d*). Together, these data show that PI3K-dependent signaling is affected by PUVA in cells other than platelets and in the clinical setting of ECP treatment.

Discussion

Despite its widespread clinical use, many aspects of PUVA's mode of action have remained uncertain. Our data show for the first time that PUVA treatment specifically inhibits the PI3K-Akt pathway by interfering with efficient recruitment of effector kinases Akt and Btk to the activated plasma membrane in response to specific stimuli. Our model (Fig. 7) suggests that psoralen-phospholipid adduct formation in the plasma membrane prevents efficient interaction between effector proteins specifically interacting with microenvironments of decreased lipid packing harboring $PI(3,4,5)P_3$.

Covalent binding of photoexcited psoralen to unsaturated fatty acids has been described before in cell-free test tubes and in cell extracts (19, 20, 24). Our mass spectra of PUVA-treated platelet extracts confirm covalent reaction with unsaturated acyl side chains. All investigated phospholipid classes formed adducts with the amotosalen, indicating no preference for the hydrophilic headgroup. Despite this seemingly unspecific photochemistry, signal transduction inhibition was remarkably specific for the PI3K pathway. Phosphorylation of Akt was decreased, but the concurrent PLC axis showed no defect even though both pathways utilize the same $PI(4,5)P_2$ substrate. Furthermore, PI3K activity was not directly affected by the presence of free amotosalen and its adducts with $PI(4,5)P_2$ because $PI(3,4,5)P_3$ levels were normal in response to platelet activation and because these particular adducts were not abundant. Consequently, specific modification of only inositides is not underlying the PI3K signal transduction defect.

Instead, PUVA inhibits normal plasma membrane recruitment of Akt and Btk in the presence of normal $PI(3,4,5)P_3$ levels, suggesting that the interaction is dependent on auxiliary facilitators. Because unsaturated fatty acids are the prime target of PUVA chemistry, such facilitators thus require normal (levels of) fatty acyl unsaturations to fulfill their role. Plasma membrane binding of small effector kinases is well studied, and even

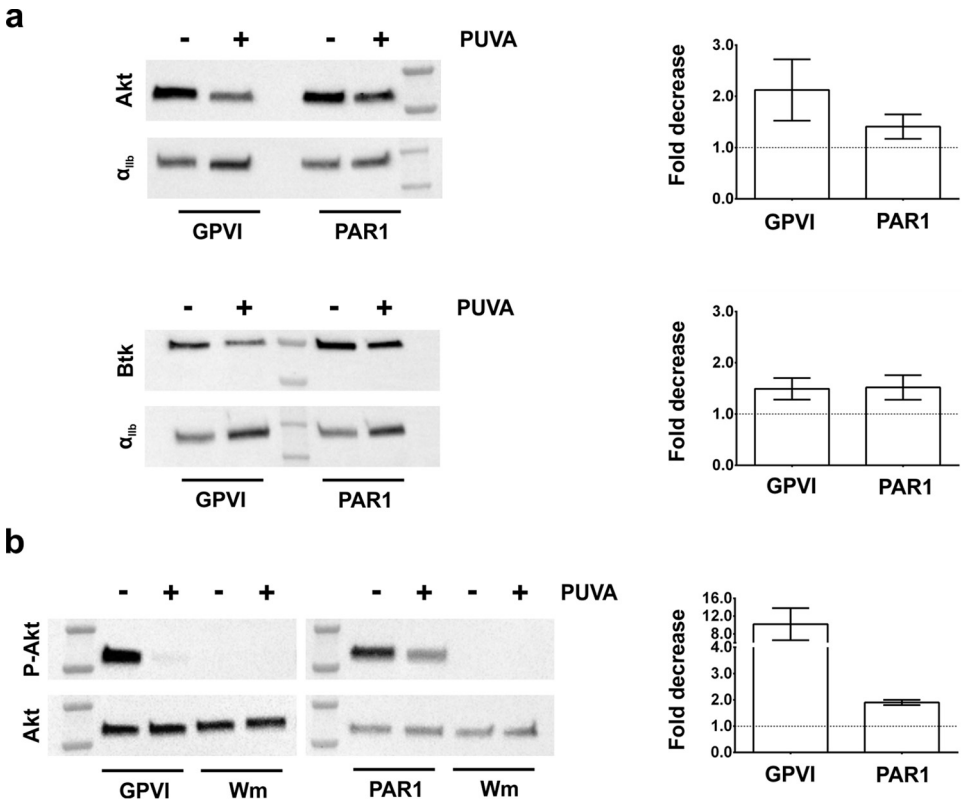

FIGURE 3. **PUVA treatment specifically affected PI3K signal transduction by impairing recruitment of Akt and Btk.** *a*, platelets were activated via the collagen GPVI or the thrombin PAR1, and the membrane fraction was analyzed by Western blotting and densitometry. Antibodies to total Akt (*Akt*) or total Btk (*Btk*) were used. Loading was controlled by reprobing with anti-integrin α_{IIb}. Molecular marker bands to the right (Akt) or in the middle (Btk) of the membrane represent molecular masses of 75 and 50 kDa. PUVA treatment *versus* control is indicated on *top* of the panels. The decrease in mean protein band density of PUVA-treated samples relative to untreated paired controls is shown in the bar graphs (mean with *error bars* representing S.D., $n = 3$). Null change is emphasized by the *horizontal dashed line*. *b*, whole lysates of activated platelets were analyzed by Western blotting and densitometry using antibodies to P-Akt. Loading was controlled by reprobing with total Akt (*Akt*). Molecular marker bands in the *left lanes* represent molecular masses of 75 and 50 kDa. To control for PI3K pathway specificity, paired experiments in the presence of 0.5 μM Wm were performed. The decrease in mean protein band density of the ratio of phosphorylated kinase to total kinase (mean with *error bars* representing S.D., $n = 6$) in PUVA-treated platelets relative to untreated paired control is shown in the bar graph. Null change is emphasized by the *horizontal dashed line*.

though it is assumed to be primarily between the PH domain sequence $KX_n(K/R)XR$ (33) and $PI(3,4,5)P_3$, additional factors (in)directly support binding. For instance, the related PH domains of PLCδ1 and GRP1 are known to harbor amino acids that penetrate the inner hydrophobic core of the membrane (34, 35). Such membrane insertion often requires the targeted membrane compartment to be less tightly packed (29, 36). Now our data show that binding of packing-sensitive probes ALPS and α-synuclein to model bilayers is hampered by PUVA. This indicates that amino acid insertion into the membrane core facilitated by unsaturated phospholipids is inhibited by PUVA. We thus hypothesize that lipid packing is the additional factor that cooperatively strengthens Akt and Btk binding as suggested by the coincidence detection (37) hypothesis of PH domain interactions with the plasma membrane. Our data provide the first proof in live cells that the acyl side chain milieu of phospholipids co-determines binding success of major PH domain-containing effector kinases in the presence of normal $PI(3,4,5)P_3$ levels.

The extent of Akt and Btk inhibition by PUVA, however, varies with the stimulus. Integrin $\alpha_{IIb}\beta_3$ activation was most affected following GPVI stimulation, less by PAR1, and not at all by PAR4. This shows that the defect is not restricted to either G-protein-coupled or immune receptor activation. It also means that the integrin conformational machinery is not affected directly by PUVA and able to respond normally if signals come in correctly from the upstream cue. How this variability in response is established, however, remains uncertain. Maybe the separate ligand-receptor circuits reside in plasma membrane microdomains of specific phospholipid composition (38) that is variably susceptible to modifications by PUVA. This follows the biochemical dogma of PI3K-dependent signaling stating that $PI(3,4,5)P_3$ molecules are scaffolding molecules restricted in space and time for controlled signalosome construction (39). The experimental setting allows activation through a single receptor-ligand couple, resulting in a distinct identifiable signal. However, in a real life physiologic environment, multiple extracellular chemicals act in concert at varying concentrations in space and time. Therefore, the net effect of PUVA on the diverse tissues that are clinically treated is difficult to predict based on our findings. However, because many signaling pathways rely on membrane recruitment, the output of PUVA-treated tissue in response to physiologically relevant chemicals will be undoubtedly altered.

In platelets, this altered output presents as delayed thrombus formation on immobilized collagen *in vitro* (23). Experimental inhibition of $PI(3,4,5)P_3$-dependent signaling in platelets indeed shows significant function defects for instance in mouse

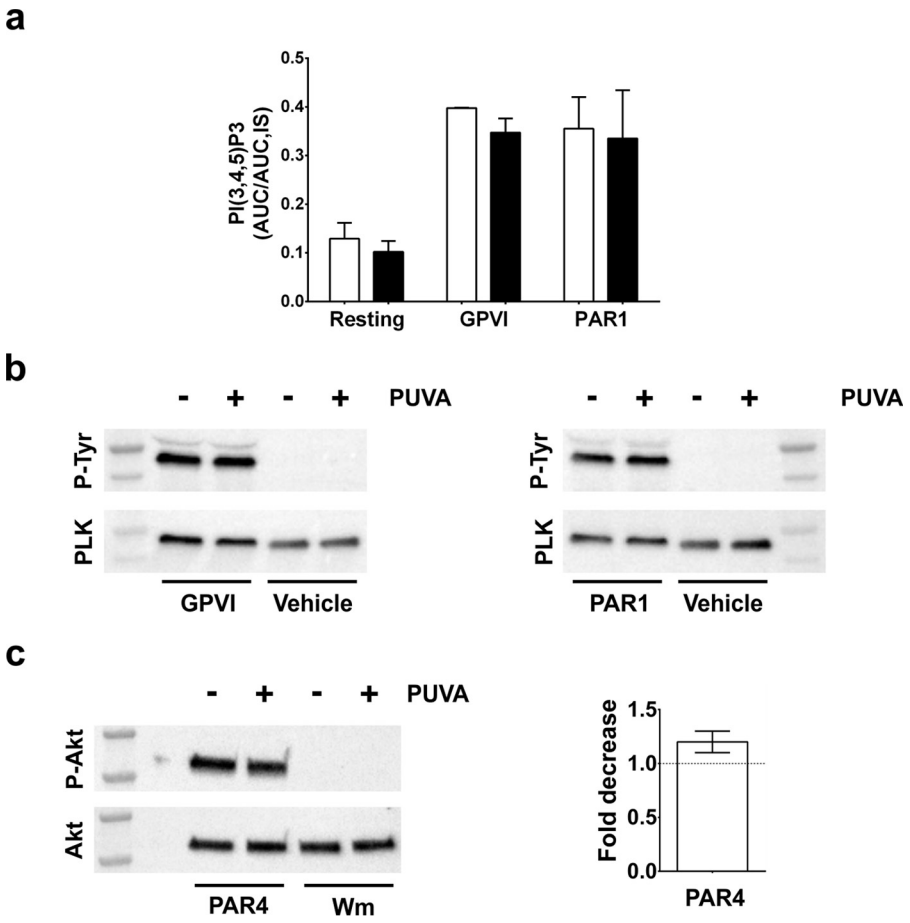

FIGURE 4. **Formation of PI(3,4,5)P_3, phosphorylation of Akt in response to PAR4 stimulation, and the phospholipase C pathway were not affected by PUVA.** *a*, the amount of PI(3,4,5)P_3(18:0/20:4) in platelet lipid extracts was determined by peak area (*AUC*) relative to that of the internal standard (*AUC, IS*). Platelets were activated via the collagen GPVI or the thrombin PAR1. Untreated controls (*open bars*) and PUVA-treated samples (*closed bars*) are shown. Resting platelets were incubated with vehicle only. Mean data and *error bars* representing S.D. are shown ($n = 4$). *b*, whole lysates of activated platelets were analyzed by Western blotting using antibodies to phosphorylated tyrosines (*P-Tyr*). Loading and specificity were controlled by reprobing with anti-pleckstrin (*PLK*) antibodies. Molecular marker bands in the *left* and *right lanes* represent molecular masses of 50 and 35 kDa. Paired control samples for resting platelets were incubated with the respective vehicle buffers. *c*, platelets were activated via the thrombin PAR4, and whole lysates were analyzed by Western blotting using antibodies to P-Akt. Loading was controlled by reprobing with total Akt (*Akt*). Molecular marker bands in the *left lanes* represent molecular masses of 75 and 50 kDa. To control for PI3K pathway specificity, paired experiments in the presence of 0.5 μM Wm were performed. The decrease in mean protein band density of the ratio of phosphorylated kinase to total kinase (mean data and *error bars* representing S.D., $n = 3$) in PUVA-treated platelets relative to untreated paired control is shown in the bar graph. Null change is emphasized by the *horizontal dashed line*.

models of Akt isoform deficiency (31), PDK1 deficiency (40), or PI3K isoform deficiency (41). In human B-cell malignancy, Btk inhibition by ibrutinib is clinically successful but increases the risk of bleeding by platelet inhibition (42). Platelets are currently treated by PUVA in certain blood banks in Europe to prevent transmission of pathogens during transfusion. This treatment efficiently reduces pathogen and white blood cell proliferation by damaging their DNA. Originally platelets were believed to be unsusceptible to PUVA because they do not contain a nucleus. Our findings have now revealed the mechanism of decreased function caused by side effects of PUVA and unrelated to DNA damage. The clinical consequences of transfusing psoralen-modified phospholipids are unknown but worthwhile investigating.

Our findings also have consequences for other fields that commonly apply PUVA. The exact biochemical drivers of PUVA's clinical success in skin pathologies or GVHD for instance remain poorly understood. We propose a substantial role for selective PI3K axis inhibition given the results of the buffy coat samples from our GVHD patient that clearly demonstrate reduced Akt phosphorylation. However, this single readout merely demonstrates attenuation of just one effector kinase (Akt), in one cell type, and to one ligand-receptor combination. The exact cellular composition of PUVA-treated tissue by type and number as well as their individual susceptibility to PUVA will eventually determine the response in a relevant physiological environment. Further study will thus require a systems approach (43) to unravel the dependence of relevant ligand-receptor couples to PUVA and combine the findings in an integrated view, ideally also taking into account effects on DNA replication and transcription where possible.

In conclusion, our research shows that PUVA selectively inhibits recruitment of kinases Akt and Btk to activated plasma membranes. This suggests that unsaturations in the plasma membrane co-determine kinase-membrane binding. We furthermore propose that the variable susceptibility of ligand-receptor couples to PUVA contributes to complex rewiring of cell

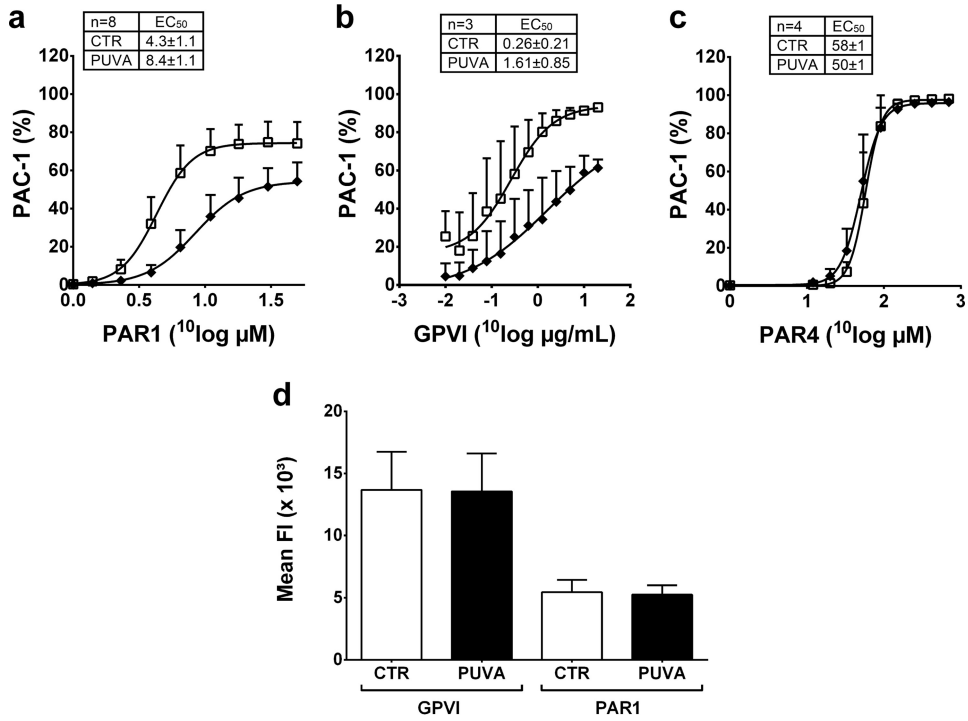

FIGURE 5. **Integrin $\alpha_{IIb}\beta_3$ activation was inhibited in PUVA-treated platelets following stimulation of GPVI and PAR1 but not PAR4 receptors.** Paired platelet samples were treated with PUVA (♦) or not (*CTR*; □) and then incubated with increasing doses of agonists to PAR1 (*a*), GPVI (*b*), or PAR4 (*c*). Activation of integrin $\alpha_{IIb}\beta_3$ was measured with flow cytometry using labeled PAC-1 antibody. The data were fitted by non-linear regression. EC_{50} values were calculated from these fits and are depicted in the *inset tables*. Data are shown as mean with *error bars* representing S.D.; the number of repeats is indicated in the *inset tables*. *d*, receptor expression levels were measured by flow cytometry. Paired platelet samples treated with PUVA or not (*CTR*) were incubated with labeled monoclonal antibodies. Median fluorescence intensities (*mean FI*) of anti-GPVI and anti-PAR1 in resting (*open bars*) and activated (*closed bars*) platelets are shown (mean with *error bars* representing S.D., $n = 3$).

and tissue fate, explaining the complexity in output and in clinical success.

Experimental Procedures

Materials—Reagents were obtained from the following sources: wortmannin (Wm), anti-phosphorylated Akt (P-Akt) (clone D25E6), anti-total (pan) Akt (40D4), anti-total Btk (C82B8), phosphotyrosine monoclonal antibody (P-Tyr-102), and secondary peroxidase-labeled antibodies (Cell Signaling Technologies, Danvers, MA); thrombin receptor PAR1-activating hexapeptide SFLLRN, 4-chloro-7-nitrobenzofurazan (NBD) chloride, tris(2-carboxyethyl)phosphine, RPMI 1640 medium without phenol red, L-glutamine, 8-MOP, and interleukin-2 (IL2) (Sigma-Aldrich); thrombin receptor PAR4-activating hexapeptide AYPGKF (Anaspec, Waddinxveen, The Netherlands); collagen receptor GPVI-activating cross-linked collagen-related peptide (University of Cambridge, Cambridge, UK); Halt protease and phosphatase inhibitor mixture (Thermo Scientific, Waltham, MA); MeSADP (Santa Cruz Biotechnology, Dallas, TX); anti-pleckstrin antibody (ab17020) and human wild type α-synuclein (ab51188) (Abcam, Cambridge, UK); and NBD iodoacetamide (IANBD) and Dynabeads human T-activator CD3/C28 (Life Technologies). All phospholipids and cholesterol were purchased dissolved in chloroform (Avanti Polar Lipids, Alabaster, AL). ALPS peptide was custom-made (Proteogenix, Schiltigheim, France) and based on the first 38 amino acids of the GMAP210 protein (44) except for the N-terminal methionine, which was mutated to cysteine to allow targeted labeling with NBD. Ficoll-Paque Premium ($d = 1.077$ g/ml at 20 °C) was obtained from GE Healthcare. Blood group AB serum was provided by the Belgian Red Cross-Flanders blood bank. The environment-sensitive NR12S probe is a Nile Red derivative and a kind gift from Dr. Klymchenko (Strasbourg University, France) (25, 26).

PUVA Treatment—PUVA treatment of platelets, liposomes, and peripheral blood mononuclear cells (PBMCs) was with the Intercept Blood System pathogen inactivation technology using amotosalen or 8-MOP as the active photosensitizing psoralen. Ultraviolet A light in the wavelength range 320–400 nm was delivered to the samples in a closed and calibrated illumination device.

Platelet concentrates for transfusion were prepared from human voluntary whole blood donations using the standardized buffy coat method (45), which is by pooling of six buffy coats and resuspension in additive solution (SSP+, Macopharma, Tourcoing, France) as described (23). To generate paired samples, two platelet concentrates were pooled, mixed, and split again in two equivalent volumes. One volume remained untreated (control), and the other was PUVA-treated in accordance with the instructions of the Intercept Blood System manufacturer (46, 47). For this, the platelet concentrate was transferred to an illumination bag while 17.5 ml of amotosalen (final 150 μM) solution was added followed by UVA illumination at a dose of 3.9 J/cm^2 for 260 s on average. Following overnight incubation on an orbital shaker at room temperature with a compound adsorption device to remove unreacted amotosalen and its photoproducts, platelet concentrates were trans-

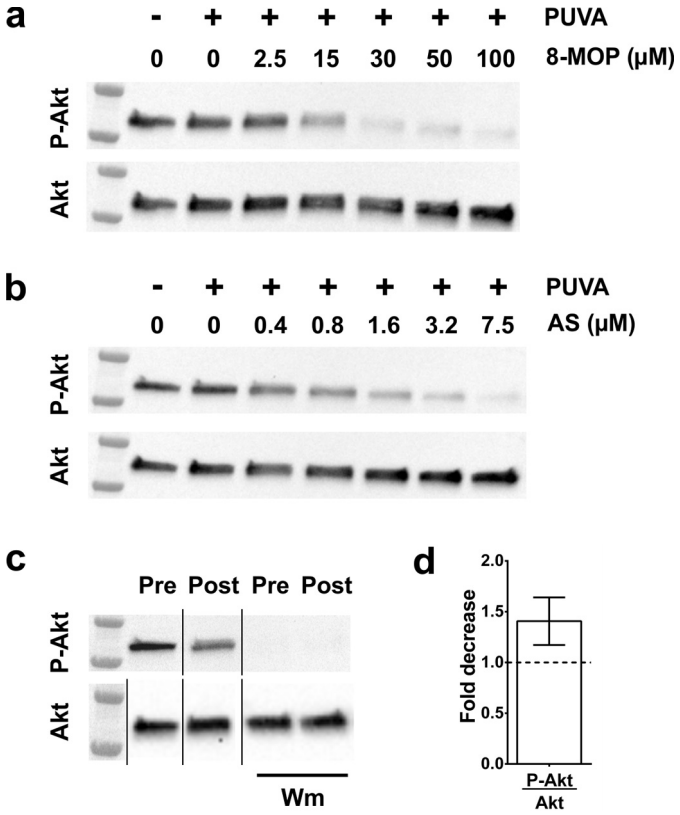

FIGURE 6. **Phosphorylation of Akt was decreased after PUVA treatment of T-lymphocytes.** *a* and *b*, dose escalations of 8-MOP (*a*) or amotosalen (*AS*) (*b*) were added to isolated PBMCs from healthy donors and subsequently illuminated with UVA light or not as indicated on *top* of each panel. The condition without psoralen contained vehicle solution and was used as a negative control. *c*, PBMCs were isolated from clinical buffy coat samples before (*pre*) and after (*post*) ECP treatment for GVHD. T-lymphocyte activation in the presence of 0.5 μM Wm was used to control for specificity of the PI3K axis. *a–c*, T-lymphocytes were activated by receptor ligation in the presence of IL2 followed by Western blotting of whole cell lysates. Antibodies to P-Akt were used, and membranes were reprobed for total Akt (*Akt*) to control for loading. Molecular marker bands in the *left lanes* represent molecular masses of 75 and 50 kDa. *d*, the mean decrease in the P-Akt over Akt signal ratio in samples post-ECP relative to pre-ECP is depicted (mean with *error bars* representing S.D., $n = 3$ different ECP treatments). Null change is emphasized by the *horizontal dashed line*.

ferred to a storage bag. Storage was under standard blood bank conditions. Experiments on platelets were performed 16–24 h after UVA illumination using low volume samples taken through sterile welded connections under a laminar flow hood.

Signal Transduction Analysis—Platelet samples were washed in Tyrode's buffer (5 mM HEPES, pH 7.4, with 136.5 mM NaCl, 2.7 mM KCl, 11.9 mM $NaHCO_3$, 0.4 mM NaH_2PO_4, 1 mM $MgCl_2$, and 0.1% (w/v) D-glucose) as described (48). Washed platelets were rested for maximally 30 min at 37 °C prior to activation with the indicated agonists and incubation times. Activation through PARs for measurement of phosphorylation downstream of PI3K activation was in conjunction with 10 μM MeSADP. Activated platelets were lysed in ice-cold buffer (50 mM Tris, pH 8.0, with 100 mM NaCl, 0.5% (v/v) octylphenoxypolyethoxyethanol (Igepal-CA630), 0.4% (w/v) sodium dodecyl sulfate (SDS), 10 mM activated Na_3VO_4, and Halt protease mixture) and mixed. Separation of platelet membrane fractions was performed by ultracentrifugation as described by Badolia *et al.* (49). In brief, following platelet activation, the reaction was stopped by the addition of Halt protease mixture (final 2×). Four freeze/thaw cycles in liquid nitrogen were performed next. Lysates were centrifuged at 1500 × *g* for 10 min at 4 °C to precipitate poorly lysed cell remnants. The supernatant was centrifuged in an ultracentrifuge at 100,000 × *g* for 30 min at 4 °C. The supernatant contained the cytosolic fraction and was kept stored at −20 °C. The pellet, which contained the membrane fraction and cytoskeleton, was rinsed with 1 ml of ice-cold Tris-buffered saline (TBS) (pH 7.4; 25 mM Tris with 150 mM NaCl and 2 mM KCl) containing 1% (v/v) Triton X-100 and 2× (final concentration) Halt protease mixture before it was resuspended in 100 μl of the same buffer. These suspensions were again centrifuged at 15,000 × *g* for 10 min at 4 °C to precipitate the cytoskeleton. The supernatant contained the membrane fraction. Sample protein concentration was determined using a bicinchoninic acid kit (Thermo Scientific, Rockford, IL).

Platelet samples (membrane fraction or whole platelet lysates) were loaded on 4–15% polyacrylamide Tris-glycine TGX gels in reducing Laemmli sample buffer. Western blotting was onto precut nitrocellulose membranes. Primary and secondary antibodies to blotted targets were prepared in TBS with 0.1% (v/v) Tween 20 and 5% (w/v) skimmed milk. Reprobing of membranes was by incubation for 30 min at 60 °C in Western reprobing buffer (50 mM Tris, pH 7.0, 2.0% (w/v) SDS, and 100 mM β-mercaptoethanol). Bound antibody was detected with enhanced chemiluminescence and an automated imaging system (ChemiDoc MP) equipped with a charge-coupled device camera and analysis software (ImageLab v4.0.1) for densitometry (all reagents, hardware, and software from Bio-Rad).

Lipid Extraction and Lipid Sample Preparation—The solvents used for the lipid extraction and LC-MS separation were HPLC grade chloroform, ultra-LC-MS grade water, and ultra-LC-MS grade methanol (Biosolve, Valkenswaard, The Netherlands). HPLC grade ammonium formate, HCl, and HPLC grade methyl *tert*-butyl ether were from Sigma-Aldrich. Phosphoinositides from platelet lipid extracts were derivatized and analyzed as described (50) with minor modifications. In brief, 3 volumes of chloroform/methanol (1:2, v/v) were added to 1 volume of platelet suspension for extraction of neutral lipids. The samples were vortex-mixed followed by centrifugation at 13,000 × *g* for 2 min. The supernatant was transferred to an LC-MS vial and used as such for analysis of phospholipids and phospholipids in complex with amotosalen. Internal standards $PI(4,5)P_2$(17:0/20:4) and $PI(3,4,5)P_3$(17:0/20:4) were added at 5 μg/ml to the remaining pellet. A volume of 1365 μl of methyl *tert*-butyl ether, methanol, and 2 M HCl (200:60:13, v/v/v) was used to resuspend the fraction followed by incubation for 15 min at room temperature with intermittent mixing. Next, 250 μl of 0.1 M HCl was added, vortex-mixed, and centrifuged at 6,500 × *g* for 2 min. The upper organic phase was transferred to a new tube, and 500 μl of prederivatization wash solution (lower phase of methyl *tert*-butyl ether, methanol, and 0.01 M HCl (100:30:25, v/v/v)) was added. The samples were again centrifuged at 6,500 × *g* for 2 min, and the upper phase was transferred for derivatization. To this, 50 μl of 2 M trimethylsilyldiazomethane in hexane was added and mixed for 10 min at room temperature followed by addition of 6 μl of glacial acetic acid (all Sigma-Aldrich) to stop the methylation reaction. Next, 500

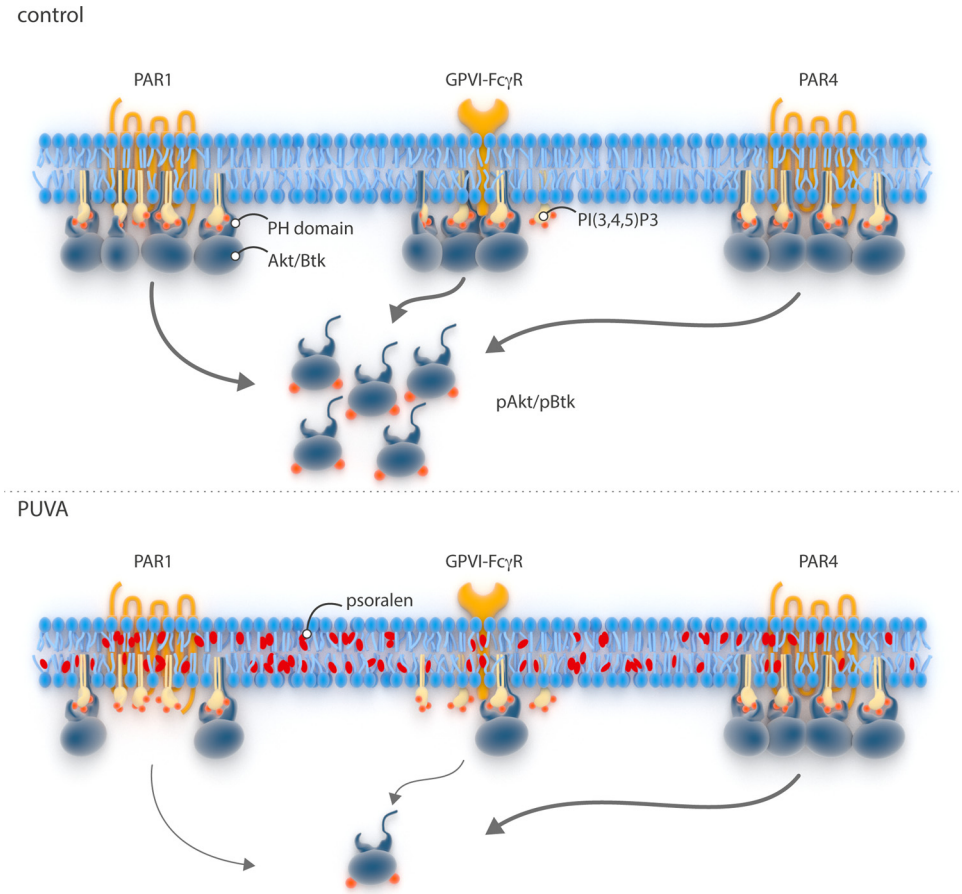

FIGURE 7. **PUVA directly interferes with PI(3,4,5)P_3-dependent processes.** Stimulation of platelet G-protein-coupled receptors like PAR1 and PAR4 or platelet immune receptors like the collagen receptor GPVI in complex with Fcγ receptor (FcγR) results in recruitment of PH domain-containing effector molecules like Akt and Btk to the spatiotemporally restricted scavenger phospholipid PI(3,4,5)P_3 in the cytosolic leaflet of the membrane. This causes phosphorylation of such targets (p*Akt/pBtk*), their release from the confined plasma membrane space, and execution of numerous cellular functions downstream. Following PUVA, however, covalent modification of unsaturated acyl side chains in all phospholipid classes attenuates efficient recruitment to PI(3,4,5)P_3 in response to certain (PAR1 and GPVI) but not all (PAR4) ligand-receptor couples.

μl of postderivatization wash solution (upper phase of chloroform/methanol/water (120:60:45, v/v/v)) was added, vortex-mixed, and centrifuged for 5 min at 1,500 × *g*. The upper phase was transferred to a high recovery glass vial and dried down in a centrifugal vacuum evaporator (MiVac duoconcentrator, Genevac, Ipswich, UK) at 37 °C. The dried sample was reconstituted in 50 μl of chloroform/methanol (1:2, v/v) before injection.

Analysis of (Phospho)lipids—Lipid analysis was based on high resolution liquid chromatography coupled to high resolution quadruple time-of-flight (TOF) mass spectrometry (51, 52). For lipidomics analyses, a 1290 Infinity LC system (Agilent Technologies, Waldbronn, Germany) was used. Lipid extracts were analyzed on an Acquity UPLC BEH Shield RP18 column (2.1 × 100 mm; 1.7 μm; Waters, Milford, MA) placed in a Polaratherm 9000 series oven (Selerity Technologies, Salt Lake City, UT) at 80 °C. Elution was carried out with a multistep gradient of mobile phase A (20 mM ammonium formate, pH 5.0) and mobile phase B (methanol) starting from 50% B to 70% B in 5 min followed by a slow gradient of 70–90% B in 30 min. Mobile phase B subsequently reached 100% in 0.1 min where it was maintained for an additional 5 min. The flow rate was 0.5 ml/min, and the injection volume was 10 μl for both positive and negative electron spray ionization (ESI) measurements. The whole system was allowed to re-equilibrate under starting conditions for 15 min. For measurement of derivatized phosphoinositides, elution was optimized using the same mobile phases at a flow rate of 1.0 ml/min, starting from 50% B to 85% B in 5 min followed by a very slow gradient of 85–90% B in 15 min. At the end of the analysis, mobile phase B reached 100% in 2 min where it was maintained for an additional 3 min. High resolution accurate mass measurements were obtained on an Agilent 6550 quadruple TOF mass spectrometer equipped with a dual Jetstream ESI source. The instrument was operated in both positive and negative ESI modes. Needle voltage was optimized to ±3.5 kV; the drying and sheath gas temperatures were set to 290 and 400 °C, respectively; and the drying and sheath gas flow rates were set to 13 and 12 liters/min, respectively. Data were collected in centroid mode from m/z 100 to 3,200 at an acquisition rate of two spectra/second in the extended dynamic range mode (2 GHz), offering an in-spectrum dynamic range of 10^5 and a resolution of ±20,000 full-width half-maximum in the lipid m/z range. MS/MS experiments were performed in targeted MS/MS mode. The quadrupole was operated at medium resolution, and the collision energy was fixed at either 20 or 35 eV. Study samples were analyzed in randomized

order. Samples were kept at 4 °C in the autosampler tray while waiting for injection.

Abundances (area under the curve (AUC)) of lipid species were extracted by the Find by Ion extraction algorithm in the MassHunter Qualitative Analysis 7.0 software package (Agilent Technologies) using predefined mass (10 ppm) and retention time extraction windows (15 s). The Agile integrator was used with an absolute peak height cutoff of 1,000 counts.

Molecular formulas, based on accurate mass, isotopic abundance, and spacing both in positive and negative ionization modes, were complemented with accurate mass database searching in an in-house-built database (populated with LIPID Metabolites And Pathways Strategy (MAPS) and Human Metabolome Database (HMDB) entries and theoretical lipid structures) and MS/MS measurement in both modes. Lipid fragmentation mechanisms and spectra in both positive and negative ionization modes were equal to those reported in the literature (52). Each lipid class displays characteristic fragment ions in positive and/or negative ESI mode. Other parameters such as lipid elution behavior and adduct formation interpretation further assisted in the identification. Regarding phosphoinositides, LC-MS cannot discriminate between PIP_2 isomers differing in the position of phosphates on the inositol ring. For trisphosphorylated PI(3,4,5)P_3, the only known isomer is PI(3,4,5)P_3. Throughout the paper, the nomenclature of the International Lipid Classification and Nomenclature Committee, *i.e.* the "comprehensive classification system for lipids," has been used (53–55).

Flow Cytometry—Membrane expression of activated integrin $\alpha_{IIb}\beta_3$ was analyzed with an acoustic focusing Attune flow cytometer (Life Technologies) using fluorescein-labeled PAC-1 monoclonal antibody (BD Biosciences). Platelets were incubated with 5% (v/v) PAC-1 and the indicated agonists or the respective vehicle buffer for 10 min at room temperature in HEPES-buffered saline, pH 7.4, with 1.0 mM $MgSO_4$ and diluted a thousand-fold immediately before readout according to previously published work (56). Signals of the isotype antibody controls were used to set threshold gates including 0.5% of 10,000 negative events. A total of 10,000 events staining positive for the platelet marker CD61 (allophycocyanin-labeled anti-CD61, Life Technologies) were measured.

Lipid Packing Analysis in Liposomes—Liposomes were prepared by mixing the (phospho)lipids from their stock solutions in chloroform and drying under nitrogen gas. Next, these were rehydrated in HKac buffer (50 mM HEPES, pH 7.2, with 120 mM potassium acetate, 1 mM $MgCl_2$, and 1 mM dithiothreitol) followed by five freeze/thaw cycles in liquid nitrogen and a 37 °C water bath. The samples were sonicated for 15 min at room temperature in a bath at 80 kHz. Liposome preparations were kept under nitrogen gas to avoid oxidation and were prepared fresh for every experiment. UVA treatment was similar to that of platelet concentrates.

The order of lipid phases was analyzed using the environment-sensitive NR12S probe (25, 26). Probe and lipid concentrations were optimized first in separate validation experiments. First, liposomes of PC(16:0/18:1) with or without 35 mol % cholesterol containing 150 μM amotosalen were UVA-illuminated or not. Next, 50 μM of liposomes by lipid content were mixed with 0.1 μM NR12S and allowed to equilibrate for 7 min in the dark at room temperature. Fluorescence was measured in a fluorescence spectrophotometer (Tecan, Männedorf, Switzerland) at 580- and 620-nm emission wavelengths using 510-nm excitation filters. The emission peak of NR12S shifts blue when partitioned to lipid phases of increased order. The fluorescence intensities at each emission wavelength were used to calculate a GP value (57). This is a relative measure between +1 (most ordered) and −1 (least ordered).

Binding experiments of the peptidic lipid-packing sensors α-synuclein and ALPS were based on the work by Vanni *et al.* (29) and Pranke *et al.* (30). First, the peptides were covalently labeled with NBD to their N termini. α-Synuclein at 1 mg/ml was labeled by incubation with 0.5 mM NBD chloride in citrate buffer, pH 7.0, with 1 mM EDTA for 24 h in the dark at room temperature. The neutral pH renders the reaction specific for the peptide N terminus, avoiding labeling auxiliary amines in the amino acid sequence (58). The reaction mixture was then re-equilibrated to HEPES-buffered saline, pH 7.4, with 5 mM KCl and 1 mM $MgSO_4$ by desalting column buffer exchange (Zeba Spin columns, Thermo Scientific). The ALPS peptide contained just one cysteine (at the N terminus) and was kept in a reducing environment (10-fold molar excess of tris(2-carboxyethyl)phosphine). Labeling was to that free N-terminal thiol using IANBD at a molar ratio of IANBD of 10:1 in HK buffer (50 mM HEPES, pH 7.2, with 120 mM potassium acetate) for 2 h at room temperature in the dark. The reaction mixture was dialyzed (membrane molecular weight cutoff, 2,000) to 4 liters of HK buffer during 24 h at 4 °C. The degree of labeling for both peptides was determined by optical absorbance at wavelengths for peptides and bound and free label.

Liposome (phospho)lipid composition was different in ALPS-NBD and α-synuclein-NBD binding experiments and was based on the literature (29). For ALPS-NBD binding, liposomes were composed of either 85 mol % PC(18:1/18:1) with 15 mol % glycerol(18:1/18:1) or 100 mol % PC(16:0/18:1) as a negative control. ALPS-NBD (0.17 μM) was added to a serial dilution of PUVA- or control-treated liposomes in HKac buffer. PUVA treatment was with 60 μM amotosalen, and unlabeled ALPS was used for background correction (F_0). Fluorescence F (emission, 535 nm) was measured at 37 °C (excitation, 485 nm). Liposomes for binding experiments with α-synuclein-NBD contained either PC(18:1/18:1) with PS(18:1/18:1) or PC(16:0/18:1) with PS(16:0/18:1) always in a 1:1 molar ratio in the presence of 50 mol % cholesterol and 10 mol % egg PC (30). Incubation, readout, and analysis were the same as for ALPS-NBD except that PUVA treatment was with 150 μM amotosalen, and the peptide concentration was 0.25 μM. Both NBD-labeled peptides were not exposed to UVA light because binding experiments were performed after PUVA.

T-cell Activation—PBMCs were prepared by Ficoll gradient centrifugation of buffy coats from healthy donors. Isolated PBMC preparations were washed three times in sterile phosphate-buffered saline, pH 7.4, by soft centrifugation to remove contaminating platelets. Finally, the cells were resuspended in

phenol red-free RPMI 1640 medium with 2 mM L-glutamine, 10 mM HEPES, and 10% (v/v) AB human serum and rested for 2 h at room temperature. The rested cells were resuspended to 40,000 leukocytes/μl in Tyrode's buffer and mixed with 8-MOP or amotosalen in a final amount of 60×10^6 leukocytes. Following PUVA, T-cells were activated in Tyrode's buffer with 2.5×10^6 CD3/CD28 human T-activator Dynabeads/10^6 leukocytes in the presence of 10 ng/ml IL2 for 30 min at 37 °C on a rotator. Cells were lysed with ice-cold lysis buffer and centrifuged at $20,000 \times g$ for 3 min. Supernatant was analyzed by SDS-PAGE Western blotting in reducing sample buffer. Cell viability was unaltered by PUVA during the course of T-cell receptor activation as monitored by Sytox Green (Life Technologies) staining in flow cytometry.

Extracorporeal Photopheresis Samples—A patient enrolled in a clinical trial for ECP at the Hospital Network Antwerp (Belgium) for the treatment of chronic GVHD gave informed consent for sampling of cells from the buffy coat suspension before and after ECP. The study was approved by the hospital's ethics committee (approval number 4591). The ECP procedure involved a leukapheresis (Spectra Optia, Terumo BCT, Lakewood, CO) yielding a buffy coat cell suspension that was diluted with saline in an illumination bag to a final 300 g by mass. 8-MOP was added to a final concentration of 0.9 μM followed by illumination in a Macogenic G2 UVA (peak wavelength, 365 nm) illumination device (Macopharma), which delivered 2 or 2.5 J/cm^2 depending on the suspension's hematocrit of $<2\%$ or $\geq 2\%$, respectively, for 10–15 min. Before and after illumination, 2-ml samples were taken aseptically from the bag for this study, and PBMCs were prepared followed by activation of T-cells as described above. A total of three independent ECP procedures were performed over a period of 2 months. Three technical replicates per sample series were performed to control for variation in SDS-PAGE Western blotting and densitometry.

Author Contributions—B. V. A. designed research, executed experiments, interpreted data, and assisted in writing the paper. R. D. executed experiments and interpreted data. R. t'K. and K. S. were responsible for mass spectrometry experiments and their data analysis and figure composition. P. Z. provided patient samples and essential patient data and interpreted data. P. V. provided essential tools and facilitated research. V. C. designed research, interpreted data, assisted in writing the paper, and managed the research team. H. B. F. designed research, interpreted data, wrote the paper, and managed research. All authors critically reviewed the manuscript and amended the text where deemed appropriate.

Acknowledgments—We thank Dr. Luk Cox and Dr. Idoya Lahortiga of Somersault1824 for scientific illustration, Davina Stabel and Dr. Jessy Lardon for help with patient sampling, Stijn De Waele and Dr. Bart Devreese for assistance with ultracentrifugation, Dr. Martine Jandrot-Perrus for supplying anti-GPVI monoclonal antibodies, Jonathan Vandenbussche for help with the lipidomics sample preparation and data processing and Dr. Pat Sandra for scientific support (both at Research Institute for Chromatography), and Dr. Andrey Klymchenko (Strasbourg University) for providing the NR12S environment-sensitive probe.

References

1. Cimino, G. D., Gamper, H. B., Isaacs, S. T., and Hearst, J. E. (1985) Psoralens as photoactive probes of nucleic acid structure and function: organic chemistry, photochemistry, and biochemistry. *Annu. Rev. Biochem.* **54,** 1151–1193
2. Lai, C., Cao, H., Hearst, J. E., Corash, L., Luo, H., and Wang, Y. (2008) Quantitative analysis of DNA interstrand cross-links and monoadducts formed in human cells induced by psoralens and UVA irradiation. *Anal. Chem.* **80,** 8790–8798
3. Pathak, M. A., and Fitzpatrick, T. B. (1992) The evolution of photochemotherapy with psoralens and UVA (PUVA): 2000 BC to 1992 AD. *J. Photochem. Photobiol. B* **14,** 3–22
4. Lin, L., Cook, D. N., Wiesehahn, G. P., Alfonso, R., Behrman, B., Cimino, G. D., Corten, L., Damonte, P. B., Dikeman, R., Dupuis, K., Fang, Y. M., Hanson, C. V., Hearst, J. E., Lin, C. Y., Londe, H. F., Metchette, K., Nerio, A. T., Pu, J. T., Reames, A. A., Rheinschmidt, M., Tessman, J., Isaacs, S. T., Wollowitz, S., and Corash, L. (1997) Photochemical inactivation of viruses and bacteria in platelet concentrates by use of a novel psoralen and long-wavelength ultraviolet light. *Transfusion* **37,** 423–435
5. Wolf, P. (2016) Psoralen-ultraviolet A endures as one of the most powerful treatments in dermatology: reinforcement of this 'triple-product therapy' by the 2016 British guidelines. *Br. J. Dermatol.* **174,** 11–14
6. Ling, T. C., Clayton, T. H., Crawley, J., Exton, L. S., Goulden, V., Ibbotson, S., McKenna, K., Mohd Mustapa, M. F., Rhodes, L. E., Sarkany, R., and Dawe, R. S. (2016) British Association of Dermatologists and British Photodermatology Group guidelines for the safe and effective use of psoralen-ultraviolet A therapy 2015. *Br. J. Dermatol.* **174,** 24–55
7. Greinix, H. T., and Knobler, R. (eds) (2012) *Extracorporeal Photopheresis*, De Gruyter, Berlin
8. Waksvik, H., Brogger, A., and Stene, J. (1977) Psoralen/UVA treatment and chromosomes. I. Aberrations and sister chromatid exchange in human lymphocytes in vitro and synergism with caffeine. *Hum. Genet.* **38,** 195–207
9. Edelson, R., Berger, C., Gasparro, F., Jegasothy, B., Heald, P., Wintroub, B., Vonderheid, E., Knobler, R., Wolff, K., Plewig, G., McKiernan, G., Christiansen, I., Oster, M., Honigsmann, H., Wilford, H., *et al.* (1987) Treatment of cutaneous T-cell lymphoma by extracorporeal photochemotherapy. Preliminary results. *N. Engl. J. Med.* **316,** 297–303
10. van Iperen, H. P., Brun, B. M., Caffieri, S., Dall'Acqua, F., Gasparro, F. P., and Beijersbergen Henegouwen, G. M. (1996) The lack of efficacy of 4,6,6′-trimethylangelicin to induce immune suppression in an animal model for photopheresis: a comparison with 8-MOP. *Photochem. Photobiol* **63,** 577–582
11. Böhm, F., Meffert, H., and Bauer, E. (1986) PUVA therapy damages psoriatic and normal lymphoid cells within milliseconds. *Arch. Dermatol. Res.* **279,** 16–19
12. Sanford, K. W., and Balogun, R. A. (2012) Extracorporeal photopheresis: clinical use so far. *J. Clin. Apher.* **27,** 126–131
13. Del Fante, C., Galasso, T., Bernasconi, P., Scudeller, L., Ripamonti, F., Perotti, C., and Meloni, F. (2016) Extracorporeal photopheresis as a new supportive therapy for bronchiolitis obliterans syndrome after allogeneic stem cell transplantation. *Bone Marrow Transplant.* **51,** 728–731
14. Laskin, J. D., Lee, E., Yurkow, E. J., Laskin, D. L., and Gallo, M. A. (1985) A possible mechanism of psoralen phototoxicity not involving direct interaction with DNA. *Proc. Natl. Acad. Sci. U.S.A.* **82,** 6158–6162
15. Zarebska, Z. (1994) Cell membrane, a target for PUVA therapy. *J. Photochem. Photobio.l B* **23,** 101–109
16. Beijersbergen van Henegouwen, G. M., Wijn, E. T., Schoonderwoerd, S. A., and Dall'Acqua, F. (1989) A method for the determination of PUVA-induced *in vivo* irreversible binding of 8-methoxypsoralen (8-MOP) to epidermal lipids, proteins and DNA/RNA. *J. Photochem. Photobiol. B* **3,** 631–635

17. dos Santos, D. J., Saenz-Méndez, P., Eriksson, L. A., and Guedes, R. C. (2011) Properties and behaviour of tetracyclic allopsoralen derivatives inside a DPPC lipid bilayer model. *Phys. Chem. Chem. Phys.* **13,** 10174–10182
18. Dardare, N., and Platz, M. S. (2002) Binding affinities of commonly employed sensitizers of viral inactivation. *Photochem. Photobiol.* **75,** 561–564
19. Frank, S., Caffieri, S., Raffaelli, A., Vedaldi, D., and Dall'Acqua, F. (1998) Characterization of psoralen-oleic acid cycloadducts and their possible involvement in membrane photodamage. *J. Photochem. Photobiol. B* **44,** 39–44
20. Li, X. Y., and Eriksson, L. A. (2005) Photoreaction of skin-sensitizing trimethyl psoralen with lipid membrane models. *Photochem. Photobiol.* **81,** 1153–1160
21. Anthony, F. A., Laboda, H. M., and Costlow, M. E. (1997) Psoralen-fatty acid adducts activate melanocyte protein kinase C: a proposed mechanism for melanogenesis induced by 8-methoxypsoralen and ultraviolet A light. *Photodermatol. Photoimmunol. Photomed.* **13,** 9–16
22. Wolf, P., Nghiem, D. X., Walterscheid, J. P., Byrne, S., Matsumura, Y., Matsumura, Y., Bucana, C., Ananthaswamy, H. N., and Ullrich, S. E. (2006) Platelet-activating factor is crucial in psoralen and ultraviolet A-induced immune suppression, inflammation, and apoptosis. *Am. J. Pathol.* **169,** 795–805
23. Van Aelst, B., Feys, H. B., Devloo, R., Vanhoorelbeke, K., Vandekerckhove, P., and Compernolle, V. (2015) Riboflavin and amotosalen photochemical treatments of platelet concentrates reduce thrombus formation kinetics *in vitro*. *Vox Sang.* **108,** 328–339
24. Caffieri, S., Zarebska, Z., and Dall'Acqua, F. (1996) Psoralen photosensitization: damages to nucleic acid and membrane lipid components. *Acta Biochim. Pol.* **43,** 241–246
25. Klymchenko, A. S., and Kreder, R. (2014) Fluorescent probes for lipid rafts: from model membranes to living cells. *Chem. Biol.* **21,** 97–113
26. Darwich, Z., Klymchenko, A. S., Kucherak, O. A., Richert, L., and Mély, Y. (2012) Detection of apoptosis through the lipid order of the outer plasma membrane leaflet. *Biochim. Biophys. Acta* **1818,** 3048–3054
27. van Meer, G., Voelker, D. R., and Feigenson, G. W. (2008) Membrane lipids: where they are and how they behave. *Nat. Rev. Mol. Cell Biol.* **9,** 112–124
28. Bigay, J., and Antonny, B. (2012) Curvature, lipid packing, and electrostatics of membrane organelles: defining cellular territories in determining specificity. *Dev. Cell* **23,** 886–895
29. Vanni, S., Hirose, H., Barelli, H., Antonny, B., and Gautier, R. (2014) A sub-nanometre view of how membrane curvature and composition modulate lipid packing and protein recruitment. *Nat. Commun.* **5,** 4916
30. Pranke, I. M., Morello, V., Bigay, J., Gibson, K., Verbavatz, J. M., Antonny, B., and Jackson, C. L. (2011) α-Synuclein and ALPS motifs are membrane curvature sensors whose contrasting chemistry mediates selective vesicle binding. *J. Cell Biol.* **194,** 89–103
31. Woulfe, D., Jiang, H., Morgans, A., Monks, R., Birnbaum, M., and Brass, L. F. (2004) Defects in secretion, aggregation, and thrombus formation in platelets from mice lacking Akt2. *J. Clin. Investig.* **113,** 441–450
32. Shattil, S. J., Hoxie, J. A., Cunningham, M., and Brass, L. F. (1985) Changes in the platelet membrane glycoprotein IIb·IIIa complex during platelet activation. *J. Biol. Chem.* **260,** 11107–11114
33. Lemmon, M. A. (2008) Membrane recognition by phospholipid-binding domains. *Nat. Rev. Mol. Cell Biol.* **9,** 99–111
34. Flesch, F. M., Yu, J. W., Lemmon, M. A., and Burger, K. N. (2005) Membrane activity of the phospholipase C-δ1 pleckstrin homology (PH) domain. *Biochem. J.* **389,** 435–441
35. Lumb, C. N., He, J., Xue, Y., Stansfeld, P. J., Stahelin, R. V., Kutateladze, T. G., and Sansom, M. S. (2011) Biophysical and computational studies of membrane penetration by the GRP1 pleckstrin homology domain. *Structure* **19,** 1338–1346
36. Bigay, J., Casella, J. F., Drin, G., Mesmin, B., and Antonny, B. (2005) ArfGAP1 responds to membrane curvature through the folding of a lipid packing sensor motif. *EMBO J.* **24,** 2244–2253
37. Carlton, J. G., and Cullen, P. J. (2005) Coincidence detection in phosphoinositide signaling. *Trends Cell Biol.* **15,** 540–547
38. Locke, D., Chen, H., Liu, Y., Liu, C., and Kahn, M. L. (2002) Lipid rafts orchestrate signaling by the platelet receptor glycoprotein VI. *J. Biol. Chem.* **277,** 18801–18809
39. Riehle, R. D., Cornea, S., and Degterev, A. (2013) Role of phosphatidylinositol 3,4,5-trisphosphate in cell signaling. *Adv. Exp. Med. Biol.* **991,** 105–139
40. Chen, X., Zhang, Y., Wang, Y., Li, D., Zhang, L., Wang, K., Luo, X., Yang, Z., Wu, Y., and Liu, J. (2013) PDK1 regulates platelet activation and arterial thrombosis. *Blood* **121,** 3718–3726
41. Gilio, K., Munnix, I. C., Mangin, P., Cosemans, J. M., Feijge, M. A., van der Meijden, P. E., Olieslagers, S., Chrzanowska-Wodnicka, M. B., Lillian, R., Schoenwaelder, S., Koyasu, S., Sage, S. O., Jackson, S. P., and Heemskerk, J. W. (2009) Non-redundant roles of phosphoinositide 3-kinase isoforms α and β in glycoprotein VI-induced platelet signaling and thrombus formation. *J. Biol. Chem.* **284,** 33750–33762
42. Byrd, J. C., Brown, J. R., O'Brien, S., Barrientos, J. C., Kay, N. E., Reddy, N. M., Coutre, S., Tam, C. S., Mulligan, S. P., Jaeger, U., Devereux, S., Barr, P. M., Furman, R. R., Kipps, T. J., Cymbalista, F., *et al.* (2014) Ibrutinib versus ofatumumab in previously treated chronic lymphoid leukemia. *N. Engl. J. Med.* **371,** 213–223
43. Mischnik, M., Boyanova, D., Hubertus, K., Geiger, J., Philippi, N., Dittrich, M., Wangorsch, G., Timmer, J., and Dandekar, T. (2013) A Boolean view separates platelet activatory and inhibitory signalling as verified by phosphorylation monitoring including threshold behaviour and integrin modulation. *Mol. Biosyst.* **9,** 1326–1339
44. Infante, C., Ramos-Morales, F., Fedriani, C., Bornens, M., and Rios, R. M. (1999) GMAP-210, a cis-Golgi network-associated protein, is a minus end microtubule-binding protein. *J. Cell Biol.* **145,** 83–98
45. Hardwick, J. (2008) Blood processing. *ISBT Sci. Ser.* **3,** 148–176
46. Irsch, J., and Lin, L. (2011) Pathogen inactivation of platelet and plasma blood components for transfusion using the INTERCEPT Blood System. *Transfus. Med. Hemother.* **38,** 19–31
47. Knutson, F., Alfonso, R., Dupuis, K., Mayaudon, V., Lin, L., Corash, L., and Högman, C. F. (2000) Photochemical inactivation of bacteria and HIV in buffy-coat-derived platelet concentrates under conditions that preserve *in vitro* platelet function. *Vox Sang.* **78,** 209–216
48. Cazenave, J. P., Ohlmann, P., Cassel, D., Eckly, A., Hechler, B., and Gachet, C. (2004) Preparation of washed platelet suspensions from human and rodent blood. *Methods Mol. Biol.* **272,** 13–28
49. Badolia, R., Manne, B. K., Dangelmaier, C., Chernoff, J., and Kunapuli, S. P. (2015) Gq-mediated Akt translocation to the membrane: a novel PIP3-independent mechanism in platelets. *Blood* **125,** 175–184
50. Clark, J., Anderson, K. E., Juvin, V., Smith, T. S., Karpe, F., Wakelam, M. J., Stephens, L. R., and Hawkins, P. T. (2011) Quantification of PtdInsP3 molecular species in cells and tissues by mass spectrometry. *Nat. Methods* **8,** 267–272
51. Sandra, K., Pereira Ados, S., Vanhoenacker, G., David, F., and Sandra, P. (2010) Comprehensive blood plasma lipidomics by liquid chromatography/quadrupole time-of-flight mass spectrometry. *J. Chromatogr. A* **1217,** 4087–4099
52. t'Kindt, R., Telenga, E. D., Jorge, L., Van Oosterhout, A. J., Sandra, P., Ten Hacken, N. H., and Sandra, K. (2015) Profiling over 1500 lipids in induced lung sputum and the implications in studying lung diseases. *Anal. Chem.* **87,** 4957–4964
53. Fahy, E., Subramaniam, S., Murphy, R. C., Nishijima, M., Raetz, C. R., Shimizu, T., Spener, F., van Meer, G., Wakelam, M. J., and Dennis, E. A. (2009) Update of the LIPID MAPS comprehensive classification system for lipids. *J. Lipid Res.* **50,** (suppl.) S9–S14
54. Fahy, E., Subramaniam, S., Brown, H. A., Glass, C. K., Merrill, A. H., Jr., Murphy, R. C., Raetz, C. R., Russell, D. W., Seyama, Y., Shaw, W., Shimizu, T., Spener, F., van Meer, G., VanNieuwenhze, M. S., White, S. H., *et al.* (2005) A comprehensive classification system for lipids. *J. Lipid Res.* **46,** 839–861

55. Liebisch, G., Vizcaíno, J. A., Köfeler, H., Trötzmüller, M., Griffiths, W. J., Schmitz, G., Spener, F., and Wakelam, M. J. (2013) Shorthand notation for lipid structures derived from mass spectrometry. *J. Lipid Res.* **54,** 1523–1530
56. Goodall, A. H., and Appleby, J. (2004) Flow-cytometric analysis of platelet-membrane glycoprotein expression and platelet activation. *Methods Mol. Biol.* **272,** 225–253
57. Kaiser, H. J., Lingwood, D., Levental, I., Sampaio, J. L., Kalvodova, L., Rajendran, L., and Simons, K. (2009) Order of lipid phases in model and plasma membranes. *Proc. Natl. Acad. Sci. U.S.A.* **106,** 16645–16650
58. Bernal-Perez, L. F., Prokai, L., and Ryu, Y. (2012) Selective N-terminal fluorescent labeling of proteins using 4-chloro-7-nitrobenzofurazan: a method to distinguish protein N-terminal acetylation. *Anal. Biochem.* **428,** 13–15

Psoralen and Ultraviolet A Light Treatment Directly Affects Phosphatidylinositol 3-Kinase Signal Transduction by Altering Plasma Membrane Packing

Britt Van Aelst, Rosalie Devloo, Pierre Zachée, Ruben t'Kindt, Koen Sandra, Philippe Vandekerckhove, Veerle Compernolle and Hendrik B. Feys

J. Biol. Chem. 2016, 291:24364-24376.
doi: 10.1074/jbc.M116.735126 originally published online September 29, 2016